



Charm Hadroproduction with an Impact Parameter Trigger

M. I. Adamovich⁶⁾, Y. A. Alexandrov⁶⁾, F. Antinori³⁾, J. L. Bailly⁵⁾, D. Barberis²⁾, W. Beusch²⁾,
A. Buys⁵⁾, M. Dameri³⁾, M. Davenport²⁾, J. P. Dufey²⁾, A. Forino¹⁾, B. R. French²⁾,
S. G. Gerasimov⁶⁾, R. Gessaroli¹⁾, F. Grard⁵⁾, R. B. Hurst³⁾, A. Jacholkowski²⁾, S. P. Kharlamov⁶⁾,
K. Knudson²⁾, J. C. Lassalle²⁾, P. Legros⁵⁾, L. V. Malinina⁶⁾, P. Mazzanti¹⁾, C. Meroni⁴⁾,
F. Muller²⁾, B. Osculati³⁾, A. Quarenì¹⁾, N. Redaelli⁴⁾, L. Rossi³⁾, G. Tomasini³⁾, D. Torretta⁴⁾,
F. Viaggi¹⁾, and M. V. Zavertyaev⁶⁾

Abstract

We report results on hadroproduction of charm based on a sample of ~ 750 D mesons. Charmed particles, produced in a thin segmented target of Si and W by a 340 GeV/c π^- beam and selected by a novel trigger with an enrichment factor of ~ 15 , are identified by the invariant mass of secondary vertices. Data were collected with the Ω' spectrometer at the CERN SPS supplemented by a silicon microstrip vertex detector. Assuming the parameterization $\sigma(\pi^- N \rightarrow DX) \sim A^\alpha$ where A is the atomic number, we find $\alpha = 0.89 \pm 0.05 \pm 0.05$ for a data sample with an average x_F of 0.2. The x_F and p_\perp distributions of the charged D mesons are also described and the possibility of a leading effect is investigated.

Contributed paper to the International Symposium on Heavy Quark Physics,

Cornell University, Ithaca, USA, June 1989

-
- 1) INFN and University of Bologna, Italy
 - 2) CERN, Geneva, Switzerland
 - 3) INFN and University of Genoa, Italy
 - 4) INFN and University of Milan, Italy
 - 5) University of Mons, Belgium
 - 6) Lebedev Physics Institute, Moscow, USSR

Hadroproduction of heavy flavours is expected to provide a useful testing ground for perturbative QCD due to the large quark masses. Hadroproduction of charm is being investigated by the WA82 collaboration using an impact parameter trigger which increases the charm content of recorded data by about a factor of 15 with respect to the 1/1000 signal-to-noise ratio of commonly used interaction triggers. The charmed particles are produced in a thin segmented target by a 340 GeV/c π^- beam and are identified by the invariant mass of secondary vertices. We present results, obtained from $\sim 25\%$ of our present data sample, on the atomic number dependence of the D production cross section and x_F and p_{\perp} distributions of charged D mesons.

The study is conducted using the Ω' spectrometer [1] at CERN whose large acceptance, particle identification capability, and good effective mass resolution are well suited to the study of charm (Fig. 1). High precision charged particle tracking and vertex reconstruction are achieved by a silicon microstrip vertex detector (MVD, see Fig. 1) which supplements the standard Ω' tracking chambers. The MVD consists of an array of four $20\mu\text{m}$ and nine $50\mu\text{m}$ pitch microstrip planes arranged in a way which facilitates triggering. It is placed together with the target on an optical bench inside the Ω' magnetic field. A telescope of eight $20\mu\text{m}$ pitch detectors is used to measure the beam position. To select multivertex events the trigger logic, executed in $\sim 350\mu\text{s}$ by the fast hardware processor MICE [2], identifies events with at least one track having an impact parameter (IP) between 0.1 and 1 mm, the range expected for charmed particles.*

Charm events have been selected from a data sample consisting of 8.8×10^6 triggers which corresponds to $\sim 10^8$ interactions in the target. This sample is $\sim \frac{1}{4}$ of the total data currently on tape. A pre-selection of the data is done using the MVD information in the x - z plane (tracks are straight lines in this projection). Events are retained which have a reconstructed primary vertex in the target and

* IP is the distance in z of a track to the primary vertex. In the Ω' reference system the z -axis is vertical along the direction of the 18 kGauss magnetic field and the x -axis is in the beam direction.

two tracks crossing downstream of the target—one track with $IP > 70\mu\text{m}$ and the other with $IP > 30\mu\text{m}$. The selected events are then reconstructed in space using the combined information of the MVD and the Ω' tracking chambers. Events are selected with reconstructed secondary vertices having the following characteristics:

1. the position of the secondary vertex is reconstructed in space outside and downstream of the target;
2. the separation between the primary and secondary vertices is $> 6\sigma$, where σ is the quadratic sum of the position measurement errors of the two vertices;
3. the total momentum vector of the secondary vertex tracks points to the primary vertex within $100\mu\text{m}$;
4. the error on the secondary vertex invariant mass is $< 12 \text{ MeV}/c^2$;
5. the lifetime of the decaying particle is $> 0.2 \text{ ps}$.

For events satisfying these criteria invariant masses are calculated assuming the secondary vertices are produced by $D^+ \rightarrow K^- \pi^+ \pi^+$, $D^0 \rightarrow K^- \pi^+$, and $D^0 \rightarrow K^- \pi^+ \pi^+ \pi^-$ (and charge conjugate) decays and taking all possible combinations of tracks (Fig. 2). Charm events are identified as those for which the invariant mass is within 3σ of the D meson mass. This sample consists of ~ 750 events with an estimated background of 20%. The Ω' particle identification capabilities have not been used in the present analysis.

Reconciling the results of charm production experiments performed with different target materials has been complicated by a lack of knowledge of the atomic number dependence of the cross section. The cross section is commonly parameterized by $\sigma \sim A^\alpha$ where A is the nuclear mass number (although it is popularly called the atomic number in the literature). In the QCD parton model the cross section is proportional to the number of quarks in the nucleus, so $\alpha \approx 1$. However, coherent effects may reduce the transparency of the nucleus and then α would be expected to approach the geometrical value of $\frac{2}{3}$. To evaluate the A dependence we have performed a measurement of the relative charm production cross sections

on silicon and tungsten. Previous evaluations of the atomic number dependence of the charm hadroproduction cross section have been made either by measuring lepton yields in beam dump experiments [3, 4] or by comparing results from various experiments, each performed with a different target material [5, 6]. Both methods are model dependent and need large corrections; and the results have shown conflicting indications. We use a segmented target which allows a direct measurement of charmed particle yields produced simultaneously on Si and W thereby minimizing systematic errors. The 1.25 mm thick target is divided along z into two equal sections. One section consists entirely of Si, the other is a sandwich consisting of a $800\mu\text{m}$ layer of W and a $450\mu\text{m}$ layer of Si. The beam is steered so that the two sections receive approximately equal intensity. The geometry of the target, reflected in the primary vertex z distribution (Fig. 3), permits a direct measurement of the ratio $\sigma_W/\sigma_{\text{Si}}$. Events within $50\mu\text{m}$ of the Si-W boundary are excluded. To correct for background contamination we assume that events outside the D peak are representative of the background under the peak. We find $\alpha_{\text{bg}} = 0.59 \pm 0.13$, a typical value for the production of light hadrons [7]. Correcting the observed numbers of events under the D peak for this background we find

$$\alpha_{\text{charm}} = 0.89 \pm 0.05 \pm 0.05.$$

The first error is statistical and the second is the systematic error arising from uncertainty in the relative beam flux on the two halves of the target.* The value of α for hadroproduction of light flavors is strongly dependent on x_F [7], defined as $\frac{p_{\parallel}}{p_{\parallel}^{\text{max}}}$ in the center-of-mass frame, and there is some indication of a similar dependence in charm production [8]. The average value of x_F for our charm sample is $\langle x_F \rangle = 0.2$; we have non-zero acceptance for all $x_F > 0$, as shown in Fig. 4. As a check, the same analysis procedure was applied to a sample of events with secondary

* The relative beam flux is obtained from the ratio of the total numbers of reconstructed primary interactions in the two halves. Beam trigger runs have been used to measure the ratio of the effective interaction probabilities in the two halves.

vertices produced by $K_s^0 \rightarrow \pi^+\pi^-$. For a K_s^0 sample with $\langle x_F \rangle = 0.05$ we find $\alpha = 0.70 \pm 0.005 \pm 0.05$ in agreement with previous measurements [7].

The EHS collaboration performed a charm production experiment using a hydrogen target and reported the observation of a leading effect, *i.e.* higher values of x_F for charm particles which contain a quark identical to one of the beam particle valence quarks [9]. This finding has neither been confirmed nor disproved. Fig. 5 shows acceptance corrected x_F distributions for our D^+ and D^- samples. The curve is of the form $(1 - x_F)^n$ where $n = 3.40 \pm 0.45$ is determined from a fit to the combined $D^+ + D^-$ distribution. The line fits the data with $\chi^2 = 6.06$ for 7 d.o.f; however, we observe a systematic difference between the two distributions, so we apply a run test [10]. From a combination of the two statistical tests we find a 10% probability for the hypothesis that the observed D^+ and D^- distributions result from the same law.

The p_\perp distribution of charm production data is often parameterized with an exponential of the form $e^{-ap_\perp^2}$. A single exponential of this form does not fit our data over the full range of p_\perp . However, the form e^{-bp_\perp} does fit the data well (see Fig. 6) and we find $b = 2.00 \pm 0.12 \text{ GeV}^{-1}$ corresponding to a mean value of p_\perp^2 of $1.5 \pm 0.2 \text{ GeV}^2/c^4$. Our p_\perp acceptance is nearly flat as shown in Fig. 7. We note that our highest observed p_\perp value (4 GeV/c) is well above those previously observed in hadroproduction.

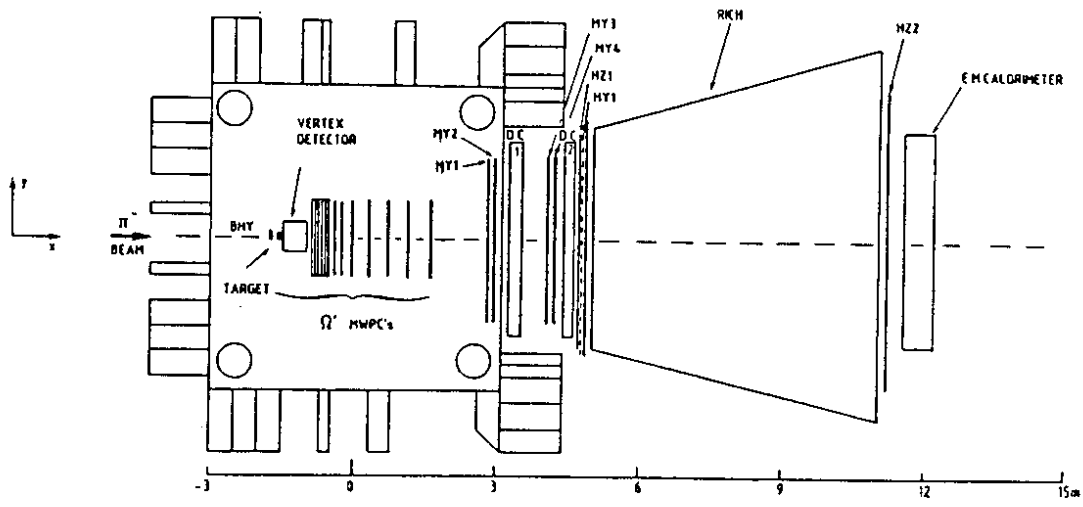
To summarize, we have measured the relative charm production cross sections of π^- on silicon and tungsten and have found that with the parameterization $\sigma \sim A^\alpha$, $\alpha = 0.89 \pm 0.05 \pm 0.05$ for $\langle x_F \rangle = 0.2$. The differential cross section $d^2\sigma/(dx_F dp_\perp^2) \sim (1 - x_F)^n e^{-bp_\perp}$ fits the data well for $n = 3.40 \pm 0.45$ and $b = 2.00 \pm 0.12 \text{ GeV}^{-1}$. There is a 10% probability that the slight excess of D^- over D^+ at $x_F \geq 0.44$ is due to a statistical fluctuation rather than to a leading effect.

REFERENCES

1. W. Beusch *et al.*, CERN/SPSC 85-62 (1985) SPSC/P218.
2. J. Anthonioz-Blanc *et al.*, CERN/DD 80-14 (1980).
3. M. E. Duffy *et al.*, *Phys. Rev. Lett.* **55** (1985) 1816.
4. H. Cobbaert *et al.*, *Phys. Lett.* **191B** (1987) 456.
5. H. Cobbaert *et al.*, *Z. Phys.* **C36** (1987) 577.
6. M. MacDermott and S. Reucroft, *Phys. Lett.* **B184** (1987) 108.
7. C. S. Barton *et al.*, *Phys. Rev.* **D27** (1983) 2580.
8. S. P. K. Tavernier, *Rep. Prog. Phys.* **50** (1987) 1439.
9. M. Aguilar-Benitez *et al.*, *Phys. Lett.* **168B** (1986) 170, *Z. Phys.* **C31** (1986) 491, *Phys. Lett.* **169B** (1986) 106.
10. W. T. Eadie *et al.*, *Statistical Methods in Experimental Physics*, North Holland Publishing Co., 1971.

FIGURE CAPTIONS

1. The Ω' spectrometer in the west hall of the CERN SPS and the silicon microstrip vertex detector.
2. Invariant masses of secondary vertex tracks for the assumptions (a) $K\pi\pi$, (b) $K\pi$, (c) $K\pi\pi\pi$, (d) sum of a-c.
3. Primary vertex position in z .
4. Global x_F acceptance for $D^\pm \rightarrow K\pi\pi$. Acceptance for D^0 is similar.
5. Acceptance corrected x_F distributions for D^+ and D^- .
6. Distribution of p_\perp of D^\pm . The line is fit to the entire distribution.
7. Global p_\perp acceptance for $D^\pm \rightarrow K\pi\pi$.



LAYOUT OF VERTEX DETECTOR

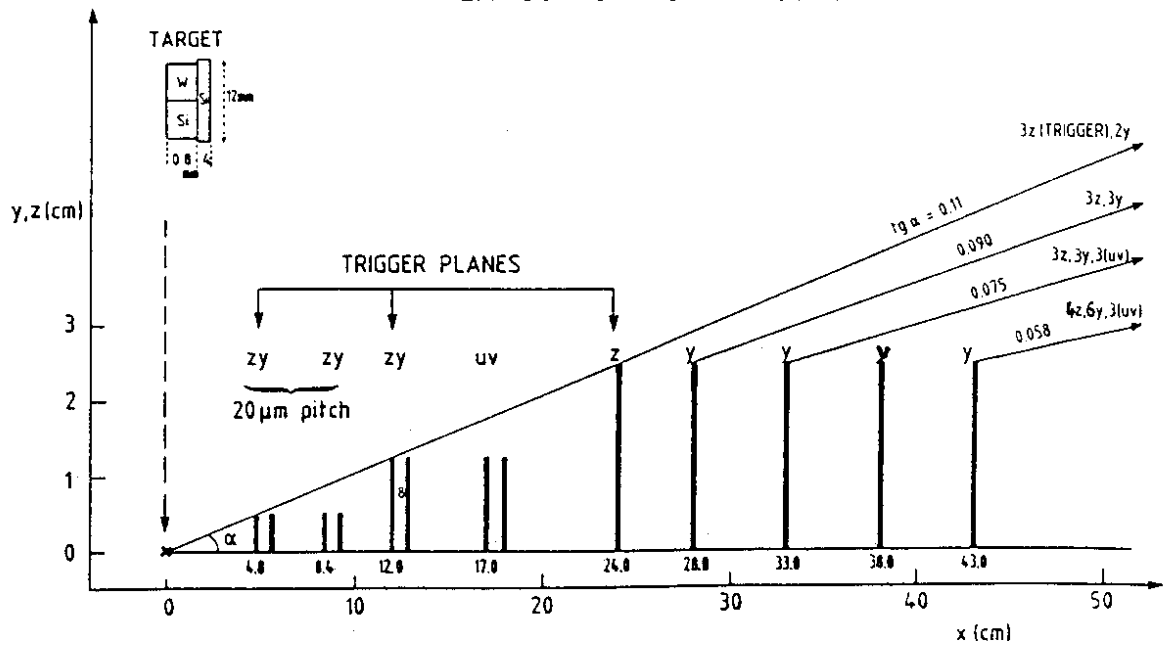


Fig. 1

WA82 ~ 20% STATISTICS

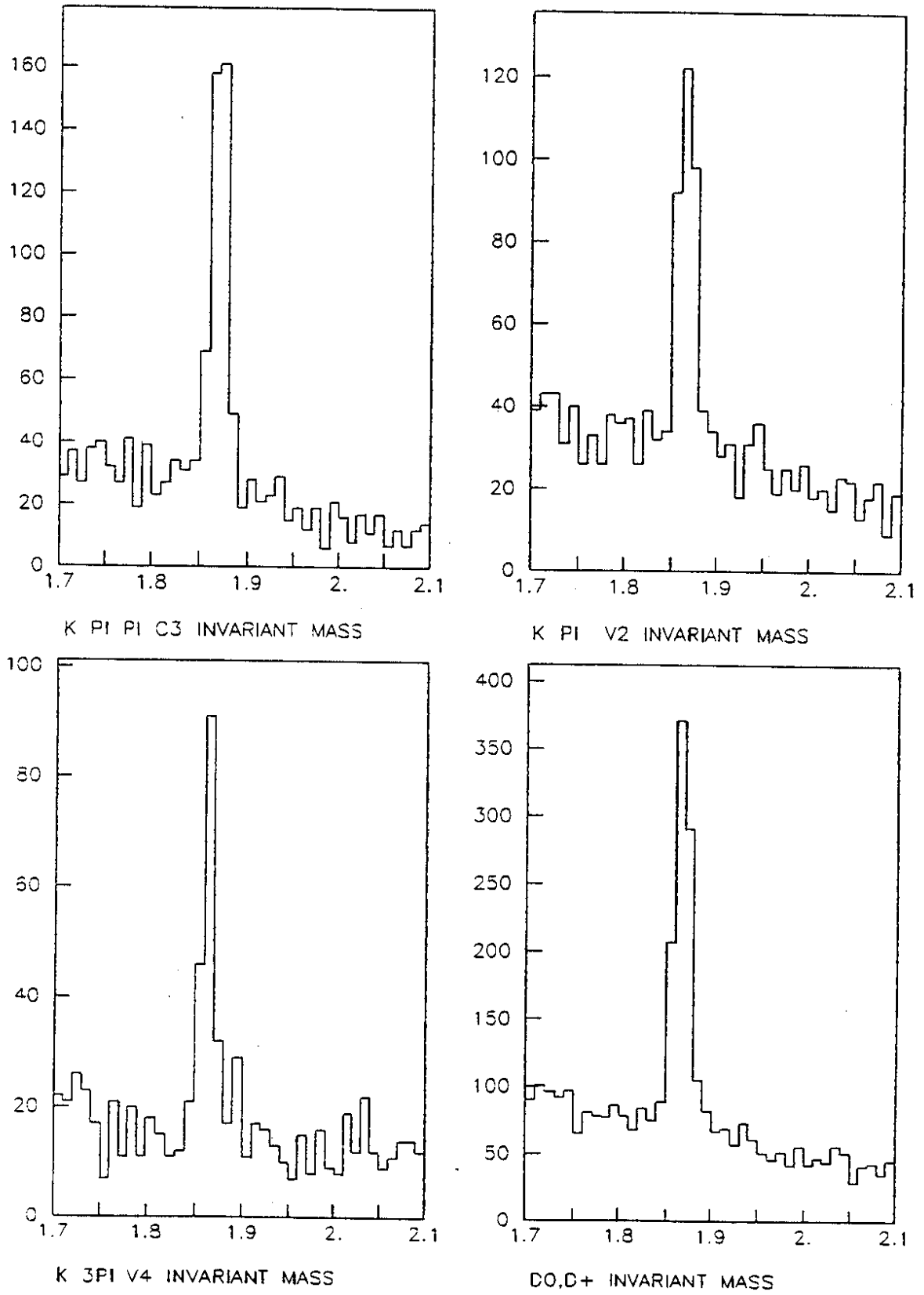


Fig. 2

$\times 10^3$

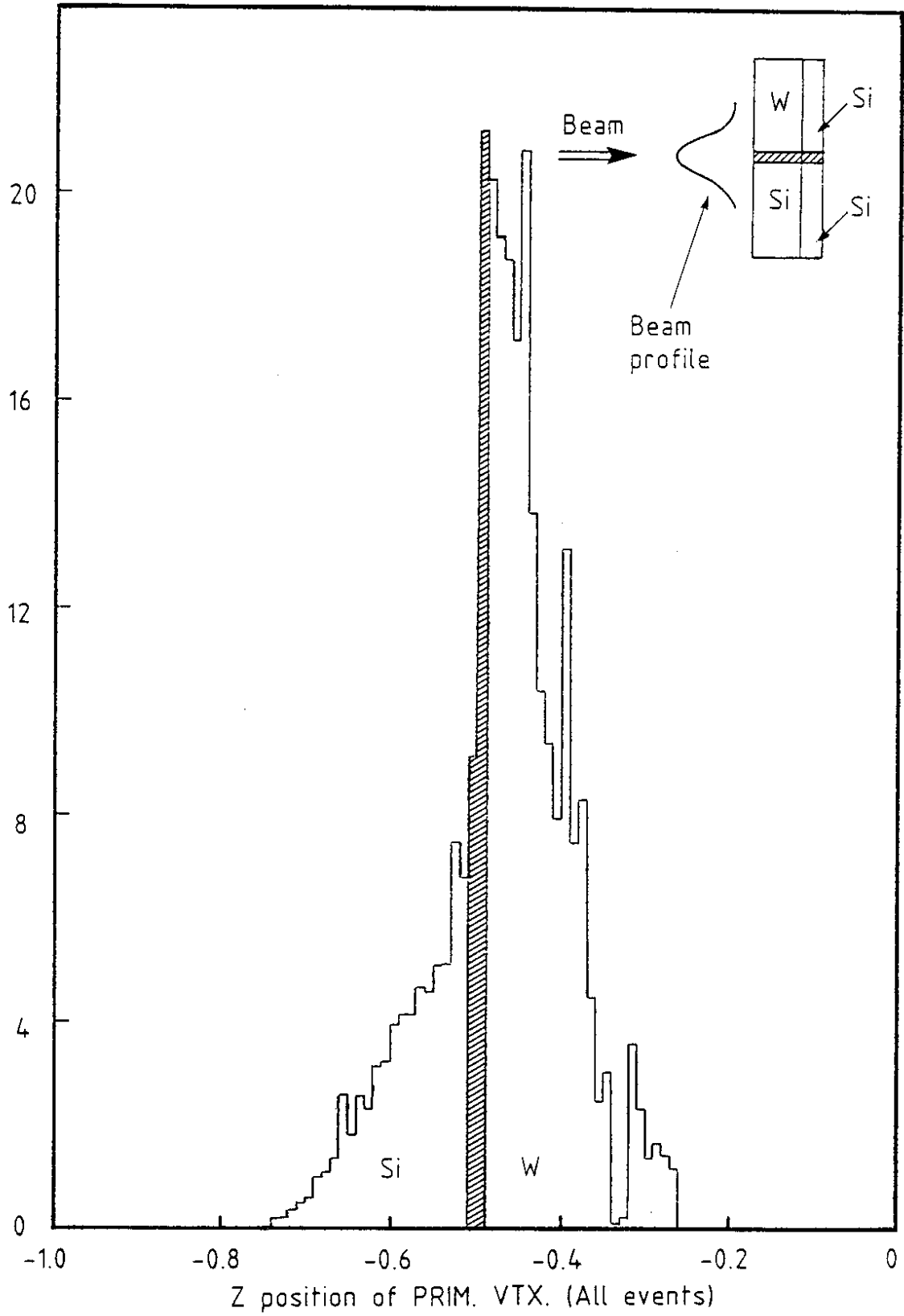


Fig. 3

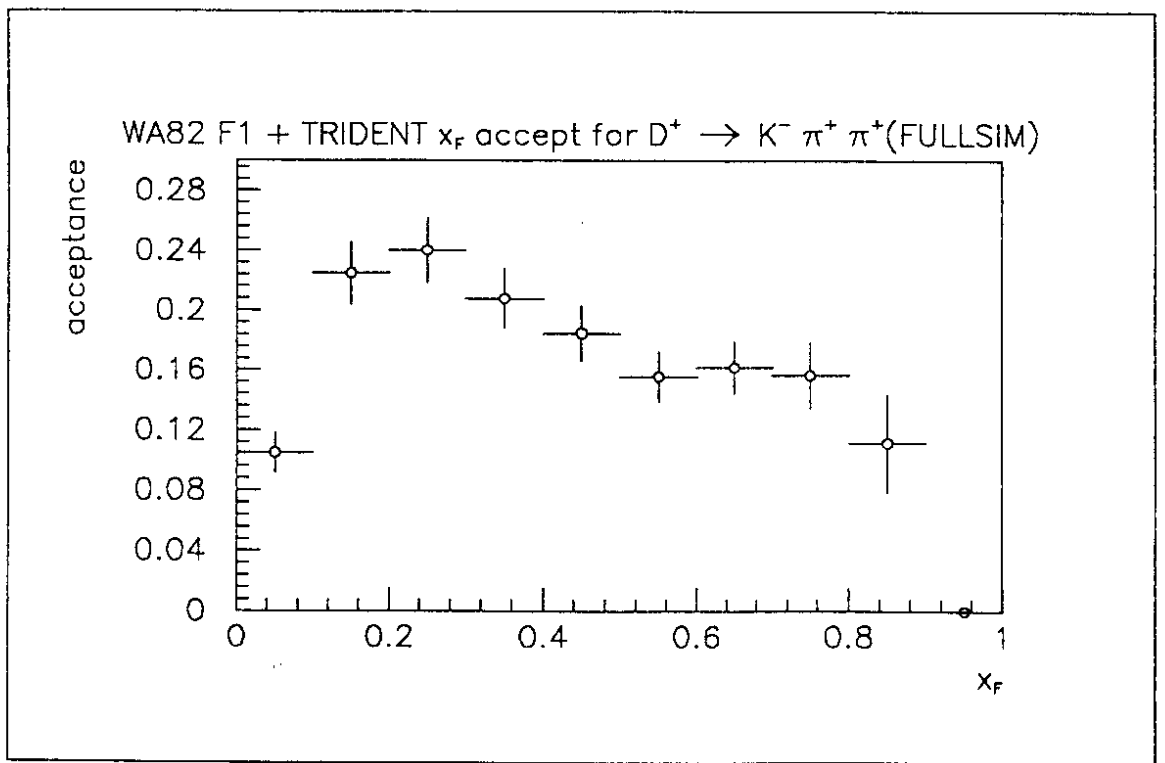


Fig. 4

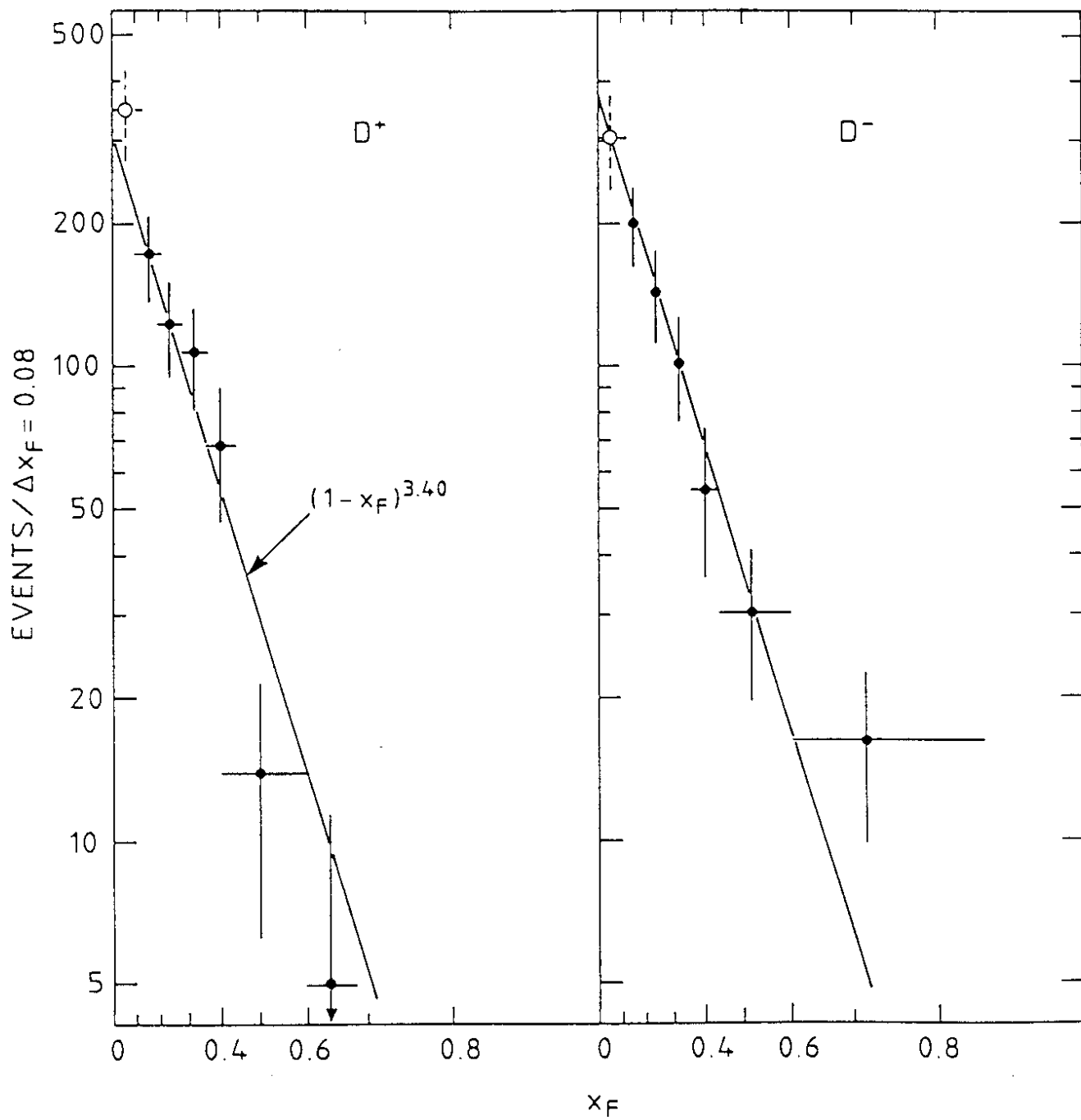


Fig. 5

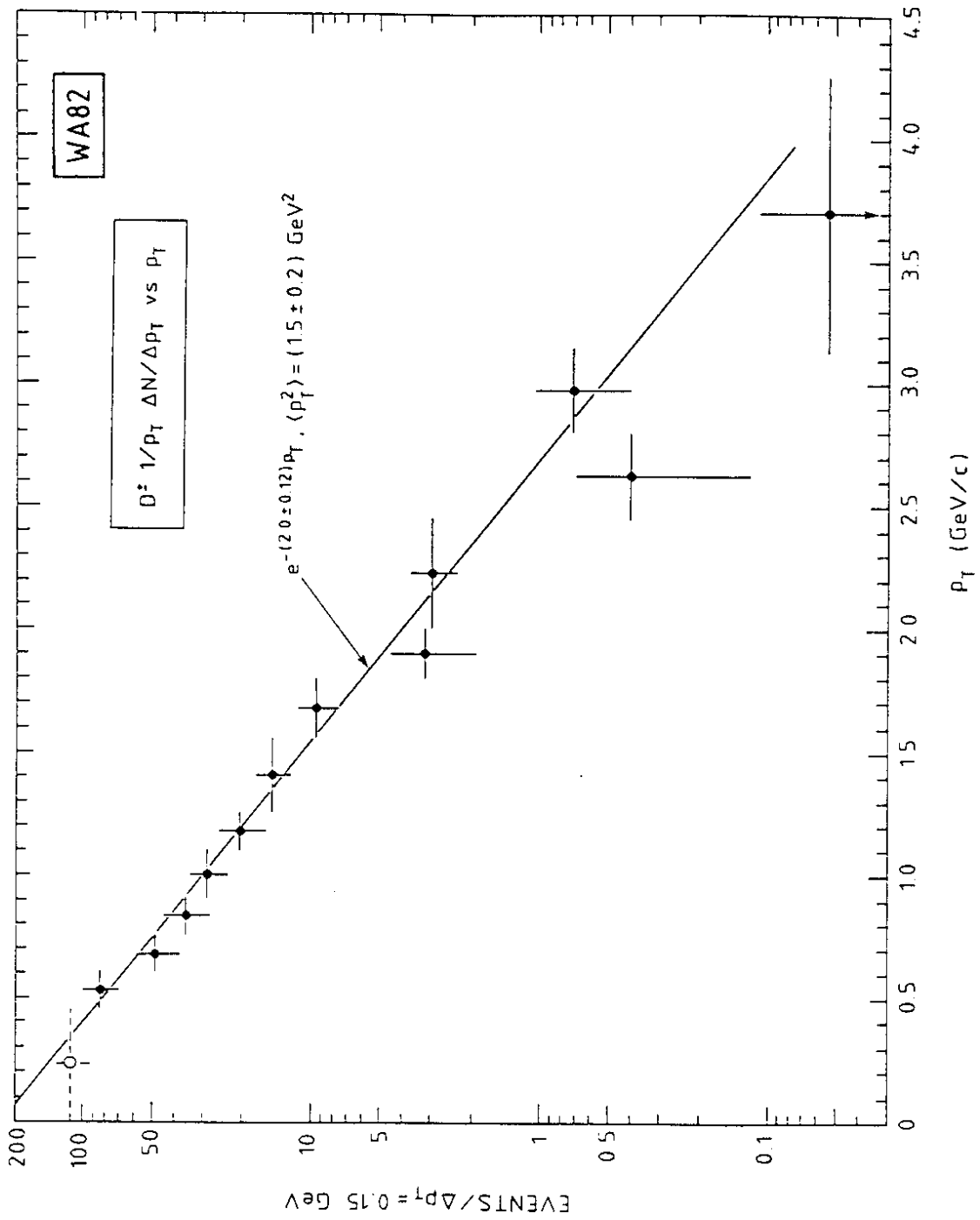


Fig. 6

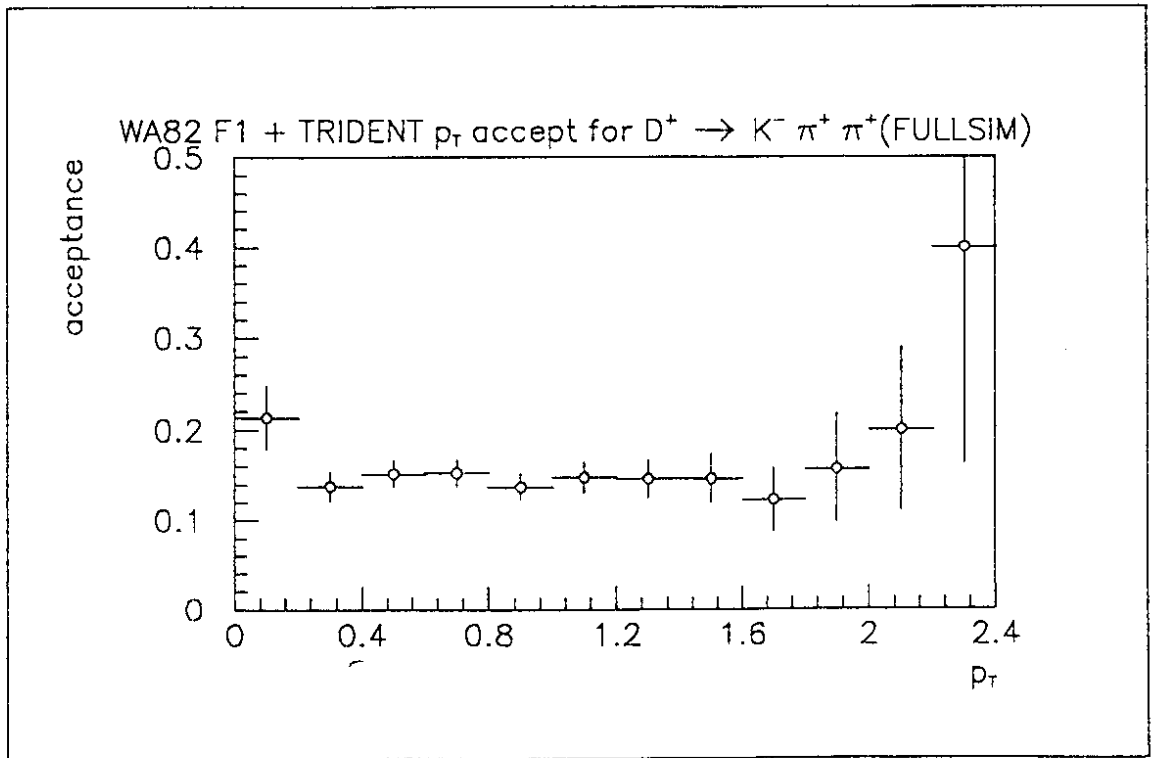


Fig. 7